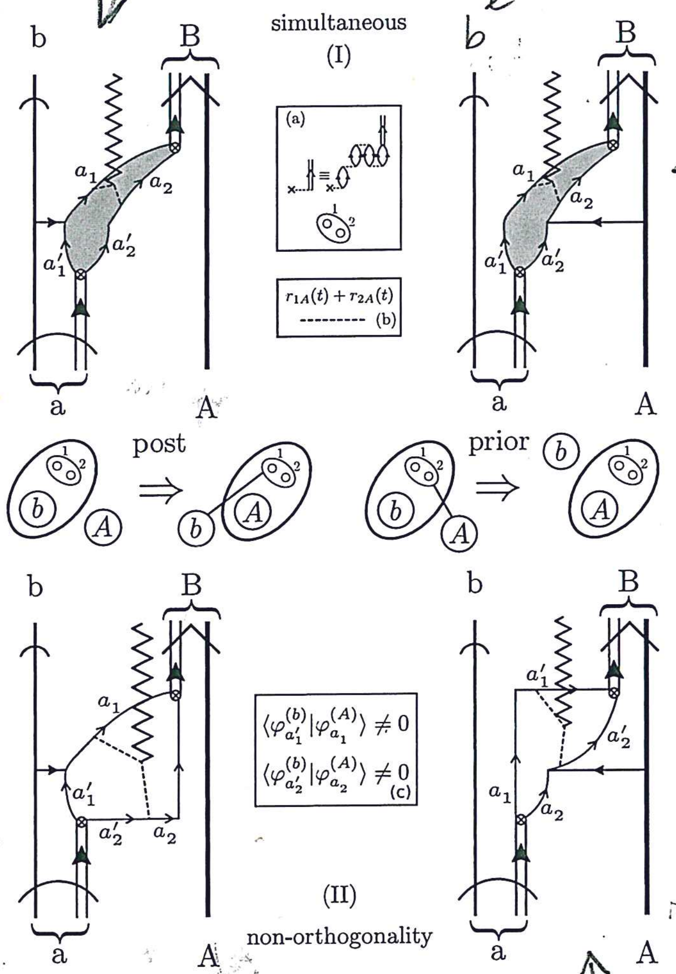

and similar for

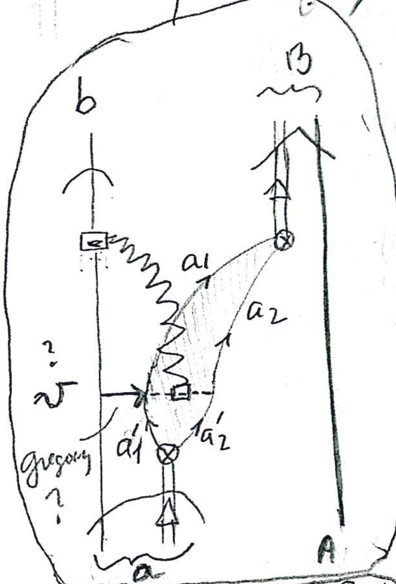

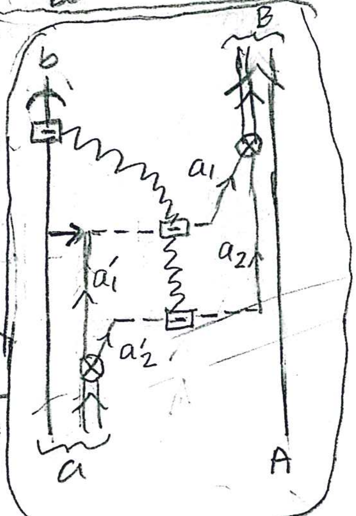

Figure 5.C.1: Graphical representation of simultaneous (I) and non–orthogonality (II) transfer processes. For details see text and cf. caption to Fig. 5.C.2.

similar for

over $f(\equiv a_1', a_2')$ and $F(\equiv a_1, a_2)$ involves a restricted number of states, namely the valence shells in nuclei B and a.

The successive transfer amplitude $\tilde{a}^{(2)}_{\infty}$ written making use of the post-prior representation is equal to (see Fig. 5.C.2 (III))

It is of notice ~~that~~ the NFT (r+s) diagrams appearing in Fig. 5.C.1 (II) are the only ones we have encountered in which to a particle-recoil coupling vertex (dashed open rectangle) and thus the starting or/and ending of a recoil mode (~~jaggy~~ jagged line) does not correspond the action of the nuclear interaction or mean field (horizontal short arrow) inducing a transfer process.

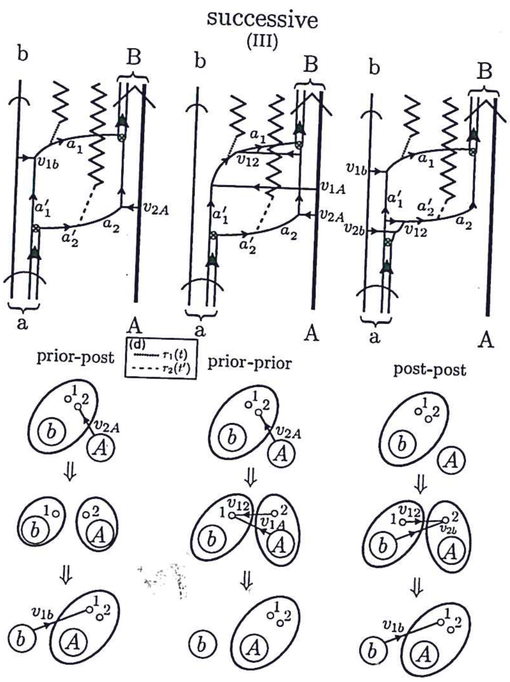

probablemente equivocada
see Fig. 1.1.3 p. 14

porqué
16/12/17

corregi

Correct

5.C.2: Graphical representation of the successive transfer of two nucleons.
tails see text.

$$
\begin{aligned}
\tilde{a}^{(2)}(\infty) = & \frac{1}{i\hbar}\int_{-\infty}^{\infty} dt(\psi^b\psi^B, (V_{bB} - < V_{bB} >)e^{i\sigma_1}\psi^f\psi^F) \\
& \times \exp[\frac{i}{\hbar}(E^{bB} - E^{fF})t + \gamma_1(t)] \\
& \times \frac{1}{i\hbar}\int_{-\infty}^{t} dt'(\psi^f\psi^F, (V_{fF} - < V_{fF} >)e^{i\sigma_2}\psi^a\psi^A > \\
& \times \exp[\frac{i}{\hbar}(E^{fF} - E^{aA})t' + \gamma_2(t)].
\end{aligned}
\tag{5.C.7}
$$

Complete with discussion pp. 443-446 Broglia Winther

$\Delta(\vec{q}_F) \sim (U_{1A}(4))^2$

To gain insight into the relative importance of the three terms contributing to Eq. (5.C.3) we discuss two situations, namely, the independent-particle model and the strong-correlation limits.

Before doing so, let us describe in some detail the graphical description of the transfer amplitudes (5.C.4) (5.C.6) and (5.C.7) displayed in Figs. 5.C.1 and 5.C.2. It is of notice that the time arrow is assumed to point upwards: (I) Simultaneous transfer, in which one particle is transferred by the nucleon-nucleon interaction (note that $U(r) = \int d^3r'\rho(r')v(|\vec{r} - \vec{r}'|)$) acting either in the entrance $\alpha \equiv a + A$ channel (prior) or in the final $\beta \equiv b + B$ channel (post), while the other particle follows suit making use of the particle-particle correlation (grey area) which binds the

see two-particle transfer p. 444 Broglia Winther pag. (pagina cuadriculada)
see also App D sect D.3 from bare to renorm

See also Sect. D.3 of App. D of Phys. Sc pp 28, 29,

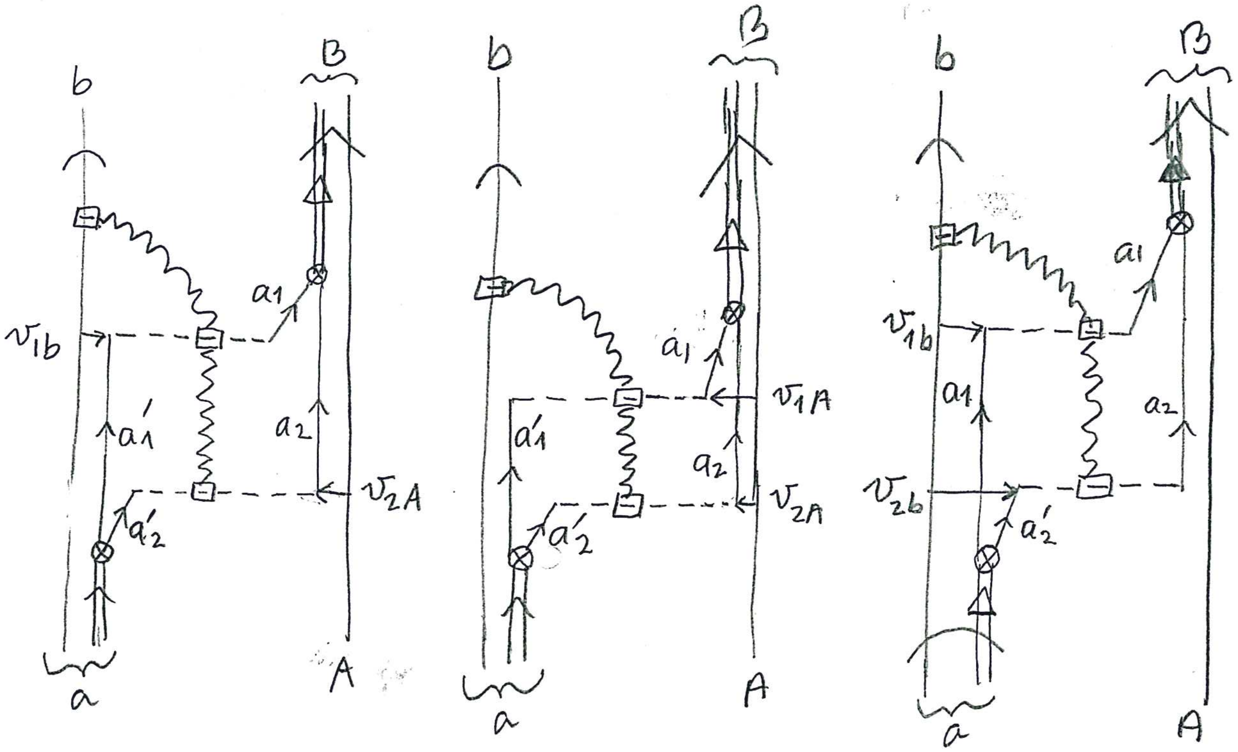

b
B
a
A
v_{1b}
v_{2A}
v_{1A}
v_{2b}
a_1
a_2
a'_1
a'_2

i	ΔL	$\sigma(^{11}Li(gs) \to {}^{9}Li(i))$ (mb) Theory	Experiment	$\theta = \theta_{cm}$
gs $(3/2^-)$	0	6.1	5.7 ± 0.9	$20° < \theta < 154.5°$
2.69 MeV $(1/2^-)$	2	0.7	1 ± 0.36	$30° < \theta < 100°$

Table 6.1.2
Integrated two-neutron transfer differential cross section associated with the reaction $^1H(^{11}Li, {}^{9}Li(i))^3H$ populating the ground state and the first excited state of ^9Li (Tanihata et al (2008), column labeled Experiment). The theoretical values are from Potel et al (2010) (see also Potel et al (2013)) & see Figs. 6.1.3 and 6.B.2).

the quadrupole and dipole collective vibrational states being exchanged ~~between~~ the two halo neutrons, ~~Also shown (left) is the diagram associated with~~ the bare nuclear pairing interaction. dashed line

	^{11}Li$(p,t)^9$Li											
	V	W	V_{so}	W_d	r_1	a_1	r_2	a_2	r_3	a_3	r_4	a_4
p, ^{11}Li $^{d)}$	63.62	0.33	5.69	8.9	1.12	0.68	1.12	0.52	0.89	0.59	1.31	0.52
d, ^{10}Li $^{b)}$	90.76	1.6	3.56	10.58	1.15	0.75	1.35	0.64	0.97	1.01	1.4	0.66
t, ^{9}Li $^{c)}$	152.47	12.59	1.9	12.08	1.04	0.72	1.23	0.72	0.53	0.24	1.03	0.83

Table 6.1.1: Optical potentials (cf. Tanihata, I. et al. (2008)) used in the calculation of the absolute differential cross sections displayed in Fig. 6.1.3, and Table 6.1.2.

We are then in presence of a paradigmatic nuclear embodiment of Cooper's model which is at the basis of BCS theory: a single weakly bound neutron pair on top of the Fermi surface of the ^{9}Li core. But the analogy goes beyond these aspects, and covers also the very nature of the interaction acting between Cooper pair partners. Due to the the high polarizability of the system under study and of the small overlap of halo and core single particle wavefunctions, most of the Cooper pair correlation energy stems, according to NFT, from the exchange of collective vibrations, the role of the strongly screened bare interaction being, in his case, minor and (see Sect. 2.6). In other words, we are in the presence of a new realization of the Cooper model in which a totally novel Bardeen–Pines–Frölich–like phonon induced interaction is generated by a self induced collective vibration of the nuclear medium.

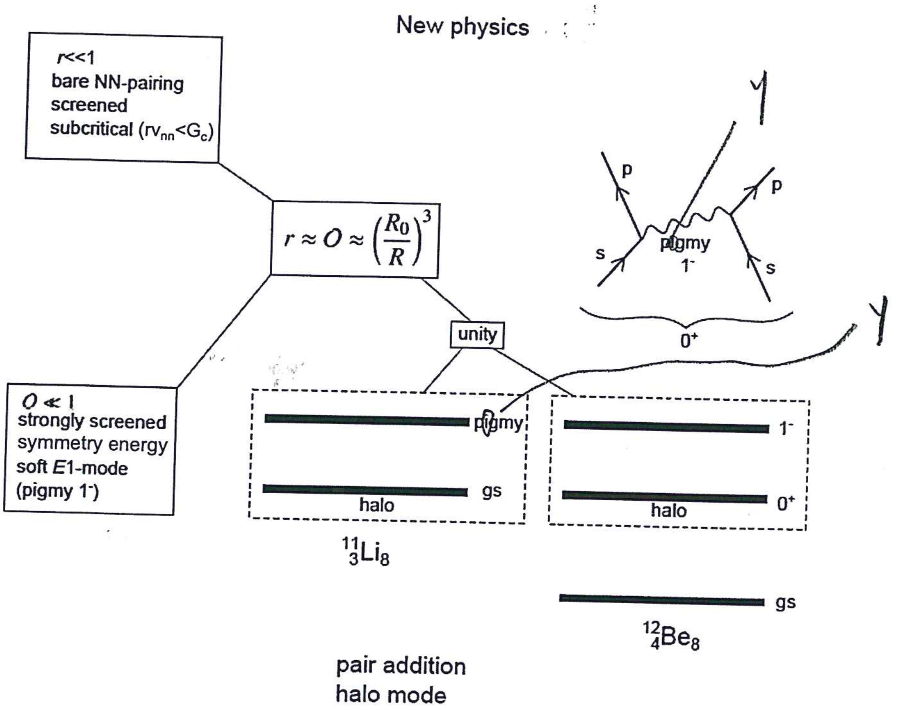

Figure 6.1.4: Schematic representation of a possible realization of halo pair addition mode in terms of the first excited 0^+ state (2.24 MeV) of ^{12}Be (for details see Sect. 2.6).

state (and the lowest $E1$–concentration strength state[9]), in other nuclei it may be an excited state which could be observed in a combined $L = 0$, and $L = 1$, two–particle transfer reaction to excited states, or in terms of $E1$ decay of the pygmy resonance built on top of it. Within this context, it is an open question whether one could expect to find a realization of such a halo pair addition mode in, for example, the first excited 0^+ state of ^{12}Be (see Fig. 6.1.4). soft mode two-neutron

Single–particle $s_{1/2}$ and $p_{1/2}$ states at threshold in neutron drip–line nuclei have been found to lead, within the framework of a bare, short range, pairing interaction scheme to halo anti–pairing effects[10]. The fact that the separation energy of the halo neutrons (halo Cooper pair) of ^{11}Li(gs) is ≈ 400keV, testifies to the fact that the anti–halo pairing effect is, in this case, overwhelmed by (dynamical) medium polarization effects.

dipole

Within this context it is of notice that, again, the interweaving of the different elementary modes of nuclear excitation, pairing and pygmy resonances in the

[9]Kanungo et al. (2015).

[10]Bennaceur, K. et al. (2000), cf. also Hamamoto and Mottelson (2003), Hamamoto, I. and Mottelson (2004).

make Xero previous versions bold face

correct xerox send to previous version cuestiones First p. curso doctorado

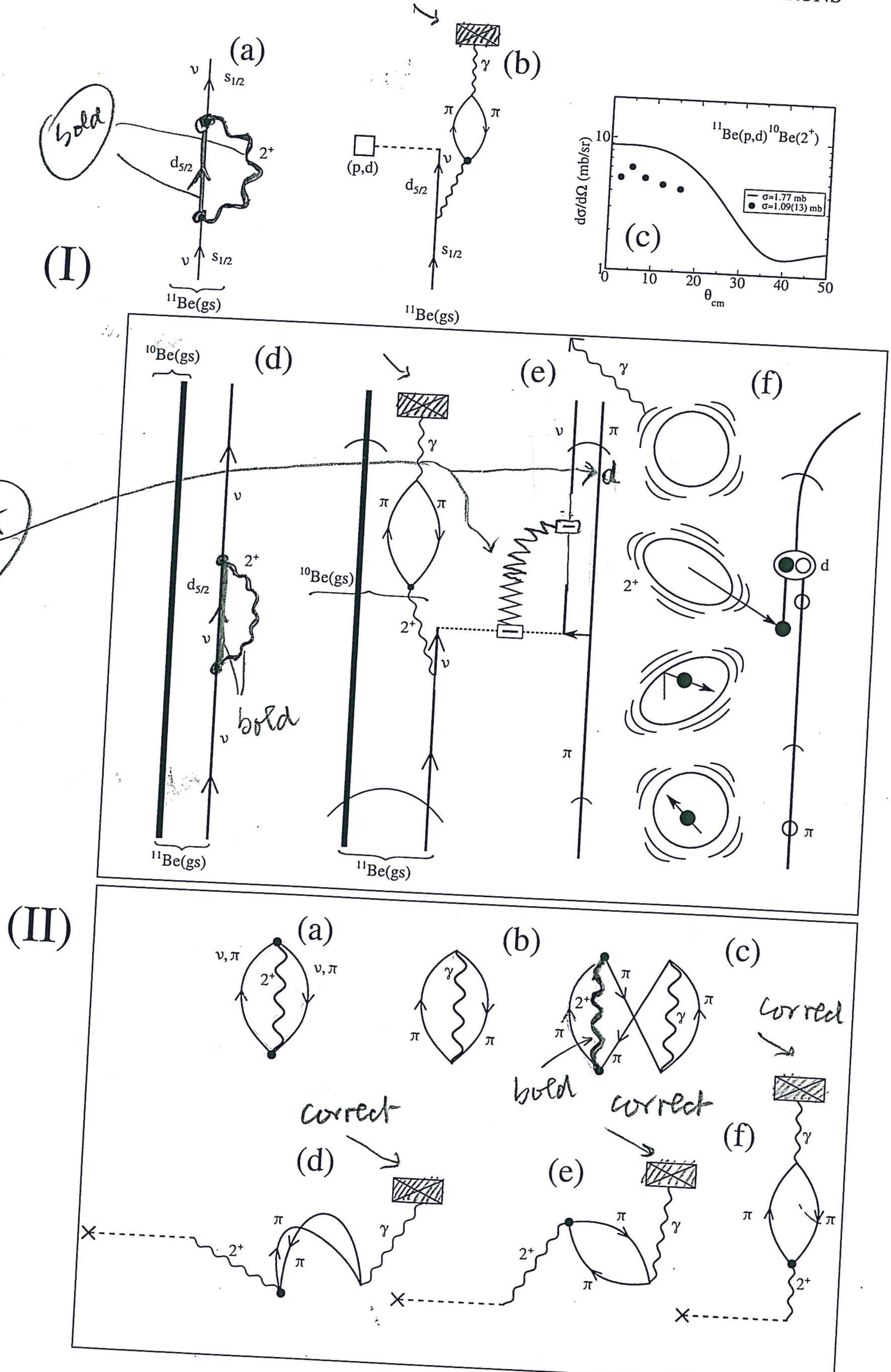

Figure 6.6.2: The reaction ^{11}Be$(p,d)^{10}$Be(2^+).

correct

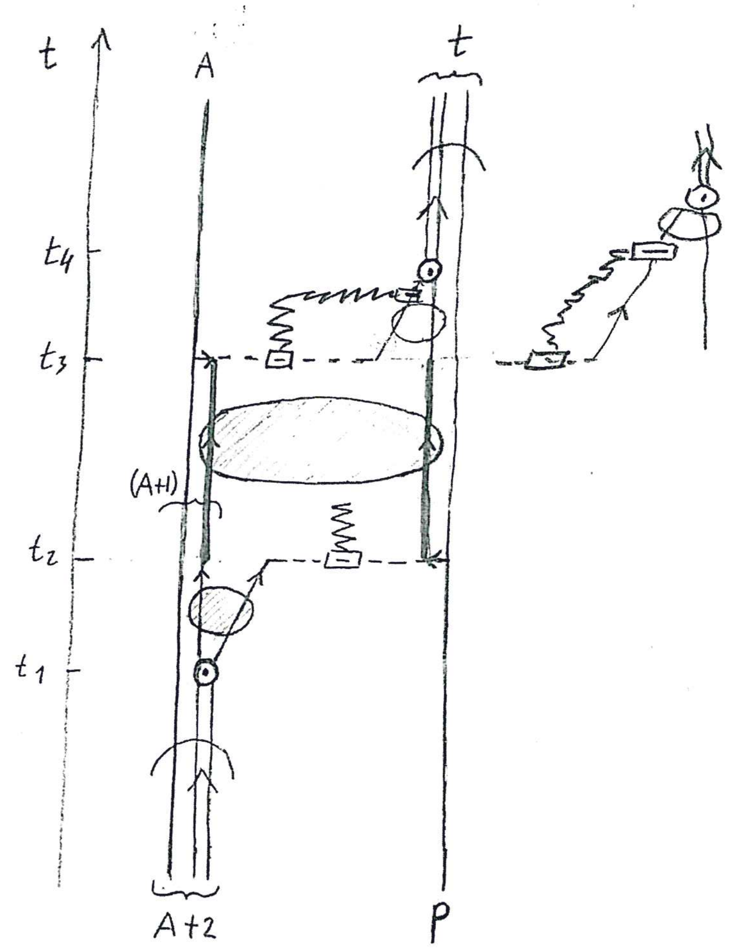

Figure 6.6.3: Diagram describing structure and reaction aspects of the main process through which a Cooper pair (di–neutron) tunnels from target to projectile in the reaction $(A + 2) + p \to A + t$. In order that the two–step process $(A + 2) + p \to (A + 1) + d \to A + t$ takes place, target and projectile have to be in contact at least in the time interval running between t_2 and t_3. During this time, the two systems create, with local regions of ever so low nucleonic presence, a common density over which the non–local pairing field can be established, and the Cooper pair can be correlated. Even with regions in which the pairing interaction may be zero. Small ellipses (with linear dimensions of the order of the nuclear radius R_0) indicate situations in which the two neutron correlation is distorted by the external mean field of a single of the systems involved of the reaction, i.e. $A + 2$ in the entrance channel, t in the exit one (see e.g. Fig. 2.6.3). The large ellipse (with linear dimensions of the order of the correlation length ξ) indicate the region in which the two partners of the Cooper pair correlate over distances of the order of the correlation length ξ. It is this information that the outgoing particle of a Cooper pair transfer process brings to the detector. In other words, this is the observable Cooper pair in terms of its specific probe, and the reason why the neutrons are described, in the interval $\Delta t = t_3 - t_1$, in terms of bold face arrowed lines.